Graphical Abstract (for review)

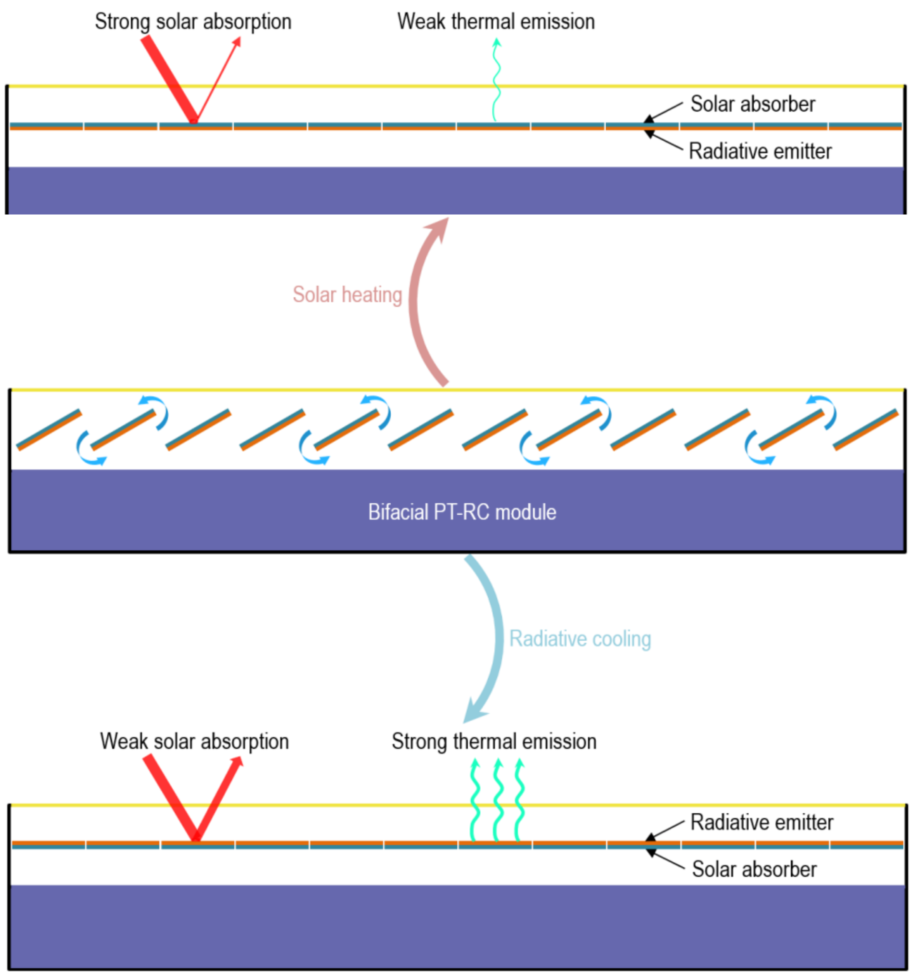

Highlights

1. A bifacial solar photothermic and radiative cooling (PT-RC) module was proposed.

2. The module can flexibly switch between solar heating and radiative cooling modes.

3. The module shows 83.3% thermal efficiency with solar irradiance of 1000 W/m^2.

4. The module reaches up to 69.9 W/m^2 net radiative cooling power.

5. Its total energy gain throughout a day is 5.36 times that of a radiative cooler.

Revised Manuscript with no changes marked

Performance analysis of a novel bifacial solar photothermic and radiative cooling module

Mingke Hu [a], Bin Zhao [b], Xianze Ao [b], Suhendri [a], Jingyu Cao [b], Qiliang Wang [c], Saffa Riffat [a], Yuehong Su [a, *], Gang Pei [b, *]

[a] *Department of Architecture and Built Environment, University of Nottingham, University Park, Nottingham NG7 2RD, UK*

[b] *Department of Thermal Science and Energy Engineering, University of Science and Technology of China, Hefei 230027, China*

[c] *Department of Building Services Engineering, The Hong Kong Polytechnic University, Kowloon, Hong Kong, China*

* Corresponding author: yuehong.su@nottingham.ac.uk; peigang@ustc.edu.cn

Abstract

Solar energy and universe coldness are two renewable and clean energy constantly sent from outer space to the earth. Solar thermal collectors and radiative coolers respectively harvest heat and cooling energy in this context. However, their static and monofunctional spectral properties mismatch energy demands in regions with large air temperature fluctuations throughout the whole year. In this work, a rotatable bifacial solar photothermic and radiative cooling (PT-RC) module capable of flexibly switch between solar heating and radiative cooling modes is proposed to realize smart thermal management. In the solar heating mode with solar irradiance of 1000 W/m^2, the PT-RC module shows 83.3% solar thermal efficiency, which is even slightly higher than that of a typical solar thermal module. In the radiative cooling mode, the PT-RC module reaches up to 69.9 W/m^2 net radiative cooling power and 11.7 °C temperature reduction. The heat and cooling energy of the PT-RC module throughout a typical day in Hefei city totals 17.7 MJ. This bifacial PT-RC module provides an alternative solution for integrating solar energy and universe coldness and shows potential in flexibly providing heat and

cooling energy in different seasons.

Keywords: *solar energy; solar photothermic; radiative cooling; rotatable; bifacial.*

1. Introduction

Solar photothermic (PT) conversion and radiative sky cooling are two environmental-friendly strategies to collect renewable energy [1, 2]. Solar thermal collectors, most of which are equipped with solar selective absorbing coatings, are designed to trap solar energy and convert it into heat [3]. Radiative sky coolers, on the other hand, work as heat dissipators by radiatively sending waste heat to the cold outer space via the "atmospheric window (8–13μm)" [4]. The building envelopes are the most familiar carrier for the solar heater and radiative cooler [5-7]. Being installed on the sunward rooftop or façade, the solar collector can deliver hot water or air to the indoor environment during cold seasons but may bring adverse effect of burdening cooling load of the building during hot days [8]. Similarly, radiative coolers are often placed on the rooftop (preferably the anti-sunward side [9]) to offer cold water or air for buildings but can cause undesired cooling effect during cold days [10]. Furthermore, solar collectors are out of operation at nighttime, rendering them incapable of work continuously. Although daytime radiative cooling has been achieved for several years attributed to great advancements in materials science [11, 12], radiative coolers are more likely to efficiently work with exemption from solar radiation, namely, at nighttime [13].

These two contrasting energy harvesting technologies, one collects heat from the universe while the other dissipates heat into it, correspond to quite the opposite spectral selectivity in the devices. A high-efficiency solar heater shows very high absorptivity in the solar radiation band (0.3–3μm) and very low emissivity in the rest wavelengths (Fig. 1A). In contrast, a high-performing radiative cooler exhibits extremely low solar absorption and strong emission within the "atmospheric window" to achieve the lowest stagnation temperature (Fig. 1B) or throughout the long-wave (above 3μm) for the highest cooling power (Fig. 1C) [14]. As most solar thermal collectors and radiative sky coolers are provided with spectrally selective coatings that are static and non-adjustable, the solar thermal collector shows poor radiative cooling capacity at night and the radiative cooler has negligible or even no solar heating effect during the daytime [15].

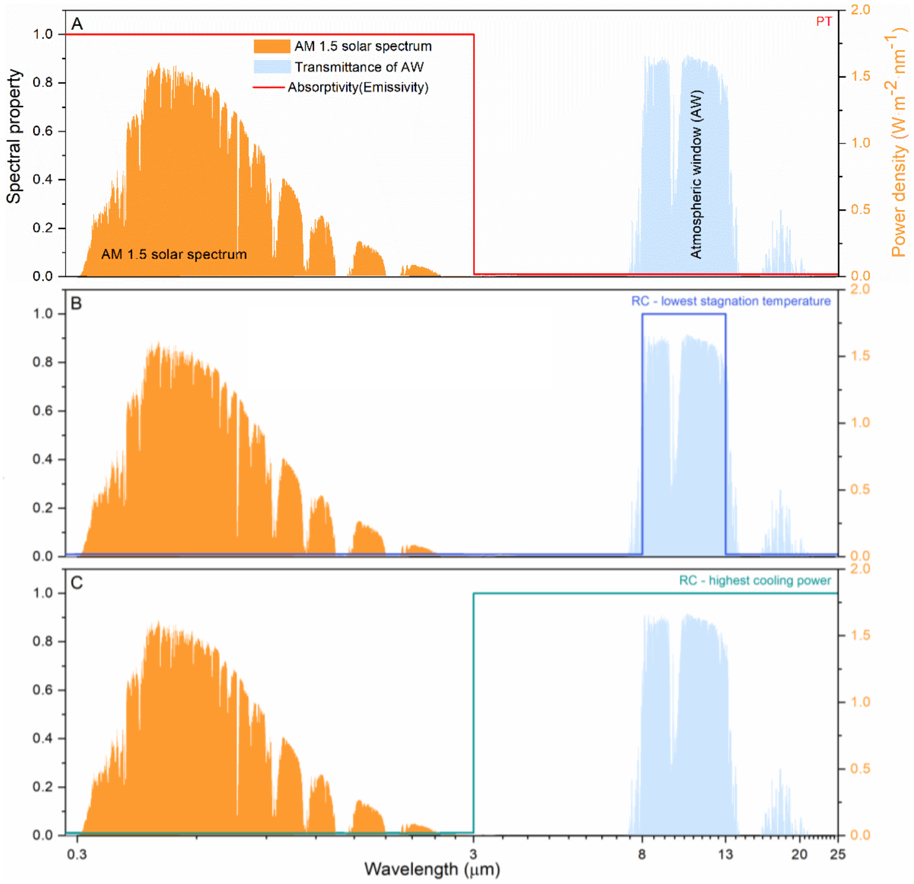

Fig. 1. Ideal spectral characteristics of different schemes. (A) solar photothermic conversion, (B) radiative cooling for the lowest stagnation temperature, and (C) radiative cooling for the highest cooling power.

With respect to the day-night and seasonal limitations of stand-alone solar thermal collection and radiative sky cooling, a few attempts have been made to develop advanced technologies in materials, structural, and systematic scales [10, 16, 17], among which combining solar photothermic conversion and radiative cooling into one single system is one of the most typical strategies [8, 18-21]. A hybrid solar photothermic and radiative cooling (PT-RC) system is capable of collecting heat in the daytime and on cold days while providing cooling energy at night and in hot seasons. The idea of combining solar heating and radiative cooling with a spectrally-coupled PT-RC coating was introduced and has been developed for years [22-24]. The ideal spectrally-coupled PT-RC coating presents unity absorptivity (emissivity) within the solar radiation band and “atmospheric window” but zero absorptivity (emissivity) excluding the two spectra, enabling itself to harvest heat during the daytime and provide cooling energy at night. However, compared to the ideal solar absorbing coating (Fig. 1A) that shows zero absorptivity (emissivity) within the “atmospheric window”, the ideal spectrally-coupled PT-RC coating has larger radiative heat loss and correspondingly lower solar thermal efficiency. Experimental results suggested that the thermal efficiency of a spectrally-coupled PT-RC collector is roughly 86% of that of a typical solar heater [23]. Unlike spectrally static solar collectors and radiative coolers, the PT-RC module equipped with a spectrally self-adaptive coating is more flexible and smarter in energy harvesting [19, 25]. On cold days the module shows relatively high solar absorption and low long-wave thermal emission to collect heat, while on hot days the module switches to the radiative cooling mode by self-adaptively lowering solar absorptivity and strengthening long-wave emissivity. However, the currently available self-tuned PT-RC module shows relatively poor performance in neither solar heating nor radiative cooling modes as the spectral selectivity in both modes is far away from the ideal ones [19, 20]. Elaborately integrating the two separated components, namely, solar absorber and radiative emitter, into a single system is another solution to achieve higher heating and cooling performance [8, 20, 26, 27]. Arranging the solar absorber and radiative cooler atop a rolling system side-by-side, Li et al. [8] devised a dual-functional device that achieved over 93% solar energy absorption in solar heating mode and up to 71.6 W/m^2 cooling power in radiative cooling mode. The glass cover used in solar collectors is a good candidate for radiative cooling due to its strong emission in mid- and far-infrared spectra. Therefore, a typical solar thermal collector can realize additional radiative cooling function at night if the glass cover is well insulated from the ambient air. Hu et al. [27] developed such a PT-RC module by adding a polyethylene (PE) film as a wind screen atop the glass cover of a flat-plate solar thermal collector. The solar absorbing panel and glass cover are respectively the solar heating component during the daytime and the radiative cooling unit during the nighttime.

In general, both a solar absorber and radiative emitter are only coated with the heating or cooling materials in one surface of the substrate, and no particular treatment is made on the opposite surface, which leaves a space for further exploitation. The concept of regulating human body temperature by using a dual-mode textile has been recently demonstrated [28]. In this study, we proposed the idea of coating the backside of the solar absorber with the radiative cooling material to achieve solar heating and radiative cooling in the same device. Such a bifacial PT-RC module can flexibly switch between heating and cooling modes by rotating the double-face coated PT-RC panel. This duality enables the module to adaptively provide thermal energy according to the dynamic end-user demands. By integrating the PT-RC module into the building envelopes, it can deliver heat on cold days and offer cooling energy in hot seasons. In addition, this dual-functional module can potentially be applied in occasions such as agriculture, industry, and vehicles where heating and cooling are alternatively required. In the following sections, we develop the structure of the bifacial PT-RC module and a mathematical model to evaluate its heating and cooling performance. Results are compared with those of the typical solar thermal collector and radiative cooler to illustrate the superiority of this PT-RC module.

2. Description of the bifacial PT-RC module

As shown in Fig. 2, the bifacial PT-RC module, mainly including a wind screen, a bifacial PT-RC panel, and an insulation layer, is arranged in flat-plate structure to integrate with building envelopes easily. The overall scale of the PT-RC module is 0.5 m in length, 0.5 m in width, and 0.08 m in height. Twelve sub-panels, each is 0.04 m in width, are made up of the bifacial PT-RC panel. Two 0.02 m-height air gaps, one is set between the PT-RC panel and the 6 μm-thick wind screen (low-density PE film) and the other between the PT-RC panel and the 0.04 m-thick thermal insulation layer, are designed to suppress non-radiative thermal loss and leave space for the panel-rotation. Each section of the bifacial PT-RC panel, with one surface coated with the solar selective absorbing coating and the

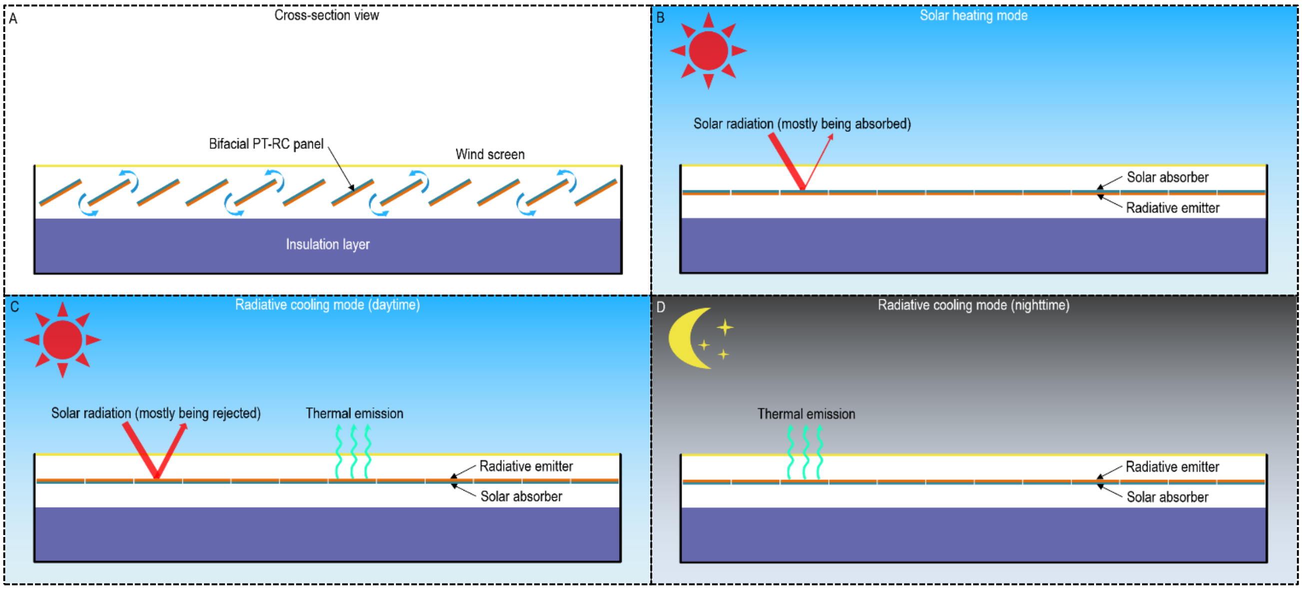

Fig. 2. Schematic of the bifacial PT-RC module. (A) Cross-section view of the module. The PT-RC module is rotatable resorting to a set of attached rotating shafts. (B) Solar heating mode, in which the solar absorber side is up-turned to absorb solar radiation. (C) Radiative cooling mode in the daytime, in which the radiative emitter side is up-turned to reject most solar radiation and emit thermal radiation. (D) Radiative cooling mode in the nighttime, in which the module is free from solar exposure and collects cooling energy.

opposite surface the radiative cooling material, is rotatable around its symmetrical axis. The PT-RC module is placed with an inclination angle of 30°. On cold days the solar absorber side is up-turned to absorb solar radiation and collect heat, while on hot days the radiative emitter side is skyward to reject solar radiation and to radiate heat to the sky. To evaluate the heating and cooling performance of the bifacial PT-RC module ("PT-RC module" for short), a solar photothermic collector (hereafter referred to as "PT module") and a radiative cooling collector (hereafter referred to as "RC module") with similar structures are employed for reference (See Fig. 3). Table 1 lists some key structural and material parameters of the three modules.

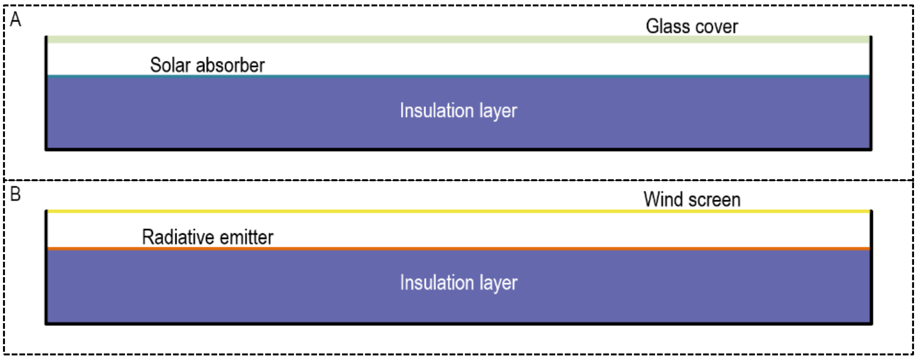

Fig. 3. Schematic of the typical (A) solar photothermic collector and (B) radiative cooling collector. Unlike the bifacial PT-RC module, these two devices have no air gap between the panel and the thermal insulation layer since the panel does not need to be rotated. Besides, the wind screen of the solar collector is a glass cover.

Table 1. Key structural and material parameters of the PT, RC, and bifacial PT-RC modules.

Components	Parameters	Values		
		PT module	RC module	PT-RC module
Whole	Length, width, and height	0.5, 0.5, and 0.06 m	0.5, 0.5, and 0.06 m	0.5, 0.5, and 0.08 m
Wind screen	Thickness	2.8 mm	6 μm	6 μm
	Transmittance (0.3–3 μm)	Based on calculation	0.88	0.88
	Emissivity (0.3–25 μm)	0.88	0.1	0.1
Panel	Absorptivity (0.3–3 μm)	0.92	0.05	0.92 (PT side) / 0.05 (RC side)
	Emissivity (0.3–25 μm)	0.1	0.9	0.1 (PT side) / 0.9 (RC side)
Insulation layer	Thickness	0.04 m	0.04 m	0.04 m
	Thermal conductivity	0.03 W/(m·K)	0.03 W/(m·K)	0.03 W/(m·K)
Air gap(s)	Height	0.02 m	0.02 m	Both 0.02 m

3. Theoretical model

A mathematical model is developed in this section to assess the heating and cooling performance of the bifacial PT-RC module and compare it with those of the two mono-functional modules. On the basis of the structure of the three modules, the mathematical model consists of three sub-models, namely, the sub-model for the wind screen, absorber/emitter panel, and insulation layer, respectively. Detailed definitions of parameters in the model are presented in the Appendix.

3.1. Wind screen

The wind screen in the PT module is a glass cover, while that in the rest two modules is a PE film. Different spectral properties of the two materials result in different heat-balance equations for the wind screen of the three modules:

$$0=\begin{cases}\alpha_{\mathrm{w}}G+h_{\mathrm{aw}}\left(T_{\mathrm{a}}-T_{\mathrm{w}}\right)+h_{\mathrm{wp}}\left(T_{\mathrm{p}}-T_{\mathrm{w}}\right)-Q_{\mathrm{rad\_sw}} & \text{PT module}\\ \alpha_{\mathrm{w}}G+h_{\mathrm{aw}}\left(T_{\mathrm{a}}-T_{\mathrm{w}}\right)+h_{\mathrm{wp}}\left(T_{\mathrm{p}}-T_{\mathrm{w}}\right)+h_{\mathrm{sw}}\left(T_{\mathrm{s}}-T_{\mathrm{w}}\right) & \text{RC and PT-RC modules}\end{cases} \tag{1}$$

3.2. Absorber/emitter panel

The spectral properties of the panel and the top-covered windscreen as well as the air gap structure of the three modules are different from each other. Thus, the heat-balance equation is expressed on a case-by-case basis:

$$0=\begin{cases}\alpha_{\mathrm{p}}G+h_{\mathrm{wp}}\left(T_{\mathrm{w}}-T_{\mathrm{p}}\right)+U_{\mathrm{ap}}\left(T_{\mathrm{a}}-T_{\mathrm{p}}\right)\pm \mathrm{Q}_{\mathrm{gain}} & \text{PT module}\\ \alpha_{\mathrm{p}}G+h_{\mathrm{wp}}\left(T_{\mathrm{w}}-T_{\mathrm{p}}\right)+U_{\mathrm{ap}}\left(T_{\mathrm{a}}-T_{\mathrm{p}}\right)-Q_{\mathrm{rad\_sp}}\pm \mathrm{Q}_{\mathrm{gain}} & \text{RC module}\\ \alpha_{\mathrm{p}}G+h_{\mathrm{wp}}\left(T_{\mathrm{w}}-T_{\mathrm{p}}\right)+h_{\mathrm{pi}}\left(T_{\mathrm{i}}-T_{\mathrm{p}}\right)-Q_{\mathrm{rad\_sp}}\pm \mathrm{Q}_{\mathrm{gain}} & \text{PT-RC module}\end{cases} \tag{2}$$

3.3. Insulation layer

The heat-balance equation for the insulation layer of the PT and RC modules is integrated into that for the absorber/emitter panel. Due to the air gap between the bifacial PT-RC panel and insulation layer, the heat-balance equation for the insulation layer for the PT-RC module is independently presented as follows:

$$h_{pi}\left(T_i - T_p\right) + U_{ai}\left(T_a - T_i\right) = 0 \qquad \text{PT-RC module} \qquad (3)$$

4. Results and discussion

Based on the developed mathematical model, the thermal performance of the bifacial PT-RC module is numerically analyzed and compared with those of the stand-alone PT and RC modules.

4.1. Solar heating mode

Firstly, the solar heating performance of the bifacial PT-RC module is investigated. The solar absorber side of the PT-RC module is up-turned in this operation mode. The thermal efficiency and the stagnation temperature under different solar irradiances are employed as two performance indicators. The ambient temperature and wind velocity are respectively set at 30 °C [29] and 2 m/s [30].

Fig. 4 illustrates the thermal efficiency of the PT and PT-RC modules at different reduced temperatures (The RC module shows no solar heating capacity). The solar irradiance is fixed at 1000 W/m^2, and the panel temperature varies from 30 to 80 °C in this case study. The thermal efficiency of both modules decreases gradually at elevated (T_p–T_a)/G value, which is because the heat loss of the module enlarges as the panel temperature increases. It is interesting to note that the thermal performance of the PT-RC module is even slightly better than that of the typical PT module. The air gap below the PT-RC panel suppresses the backside heat loss, partly contributing to the thermal performance advantage of the PT-RC module, particularly at large (T_p–T_a)/G value. Another reason why the PT-RC module is superior to the PT module in solar heating performance is the difference in spectral properties of the two wind screens, namely, the glass cover in the PT module and the PE film in the PT-RC module. The glass cover shows very high long-wave absorptivity and emissivity, indicating that it will absorb a significant part of radiant heat from the solar absorber. This part of radiant heat will be radiatively sent to the sky and convectively dissipated to the local surroundings. In contrast, the PE film exhibits very low long-wave absorptivity and emissivity, signifying that a tiny portion of radiant heat from the solar absorber will be absorbed and dissipated by it, although a fraction of heat is directly transferred from the solar absorber to the sky.

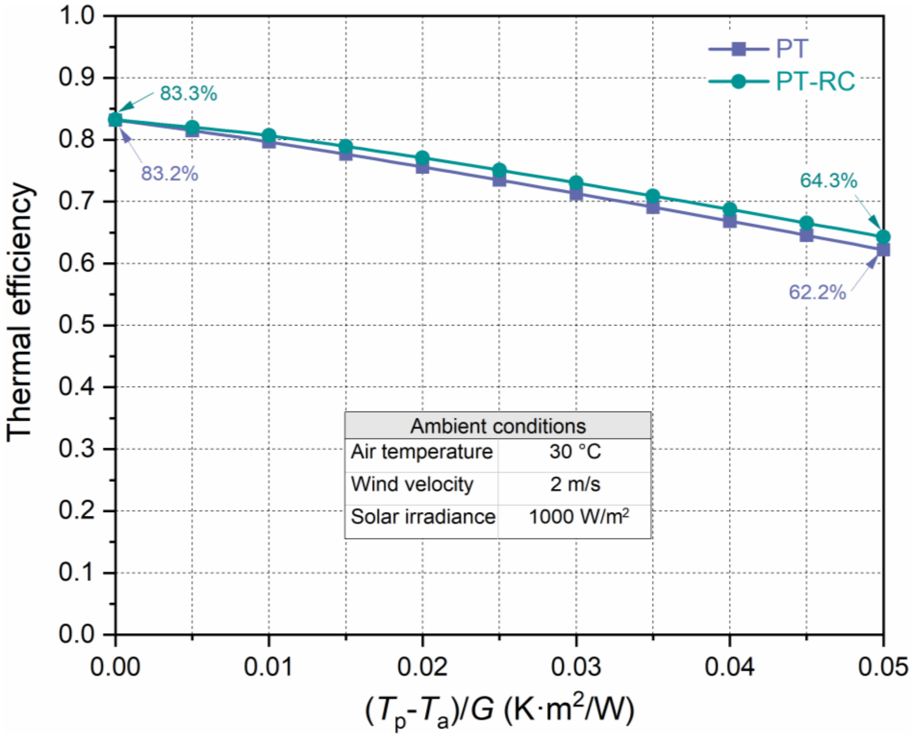

Fig. 4. Solar thermal efficiency of the PT and PT-RC modules under different panel temperatures. The ambient temperature, wind velocity, and solar irradiance are respectively set at 30 °C, 2 m/s, and 1000 W/m^2.

However, the superiority of the PT-RC module in thermal efficiency at higher panel emissivity (0.3–25 μm) will be dwindled or even vanished. The thermal emission of the solar absorber will be strengthened with increased long-wave emissivity, in which case the glass cover in the PT module can block the direct heat exchange between the absorber and sky, while the PE film in the PT-RC module will allow most thermal emission to pass through it. This assertion is demonstrated in Fig. 5. Though the PT-RC module shows higher thermal efficiency when the panel emissivity (0.3–25 μm) is very low (The panel absorptivity within 0.3–3 μm remains at 0.92), its thermal performance deteriorated rapidly as the panel emissivity increases. In contrast, the PT module is much less sensitive to the panel emissivity due to the existence of the longwave-opaque glass cover, resulting in higher thermal efficiency when the panel emissivity exceeds a critical point (e.g., points 0.12, 0.25, and 0.22 in Fig. 5). The glass cover of the PT module mainly serves as a radiative heat barrier above the critical point that promotes thermal efficiency while mainly acts as a radiative heat dissipater below the critical point that detracts thermal efficiency. As the solar absorber is commonly covered with a solar selective absorbing coating which shows emissivity less than 0.1 (see the orange zone in Fig. 5), the PT-RC module performs better than the PT module in solar heating, regardless of the mechanical strength of the PE film.

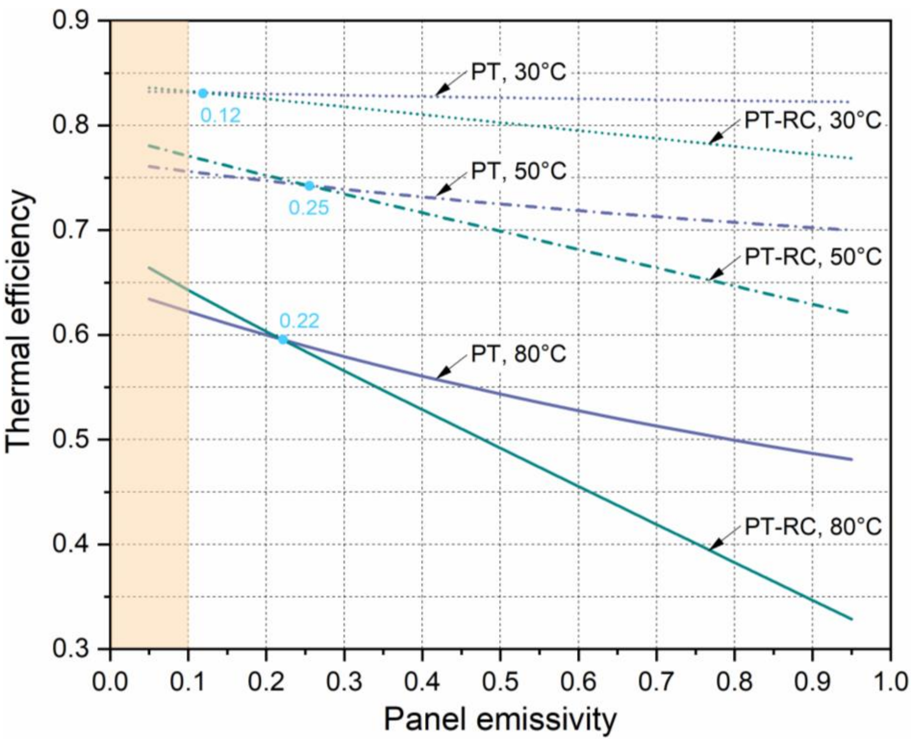

Fig. 5. Solar thermal efficiency of the PT and PT-RC modules under different panel temperatures and panel emissivity (0.3–25 μm). The ambient temperature, wind velocity, and solar irradiance are respectively set at 30 °C, 2 m/s, and 1000 W/m^2.

Panel stagnation temperature is another key performance indicator representing the highest or lowest possible temperature a panel can reach under given conditions. Therefore, panel stagnation temperature of the PT and PT-RC modules in solar heating mode is compared in addition to thermal efficiency. As shown in Fig. 6, the panel stagnation temperature of the PT-RC module is slightly above that of the PT module under each solar irradiance. It is worth pointing out that the stagnation temperature difference between the two panels enlarges with increasing solar irradiance. Higher solar irradiance corresponds to greater panel-ambient temperature gap and thus more heat loss. However, the air gap below the PT-RC panel helps block more backside heat loss, especially at higher panel temperatures. Besides, as long-wave absorptivity and emissivity of the glass cover are much higher than those of the PE film, radiative heat loss of the PT module is increasingly greater than that of the PT-RC module with the increase in solar irradiance.

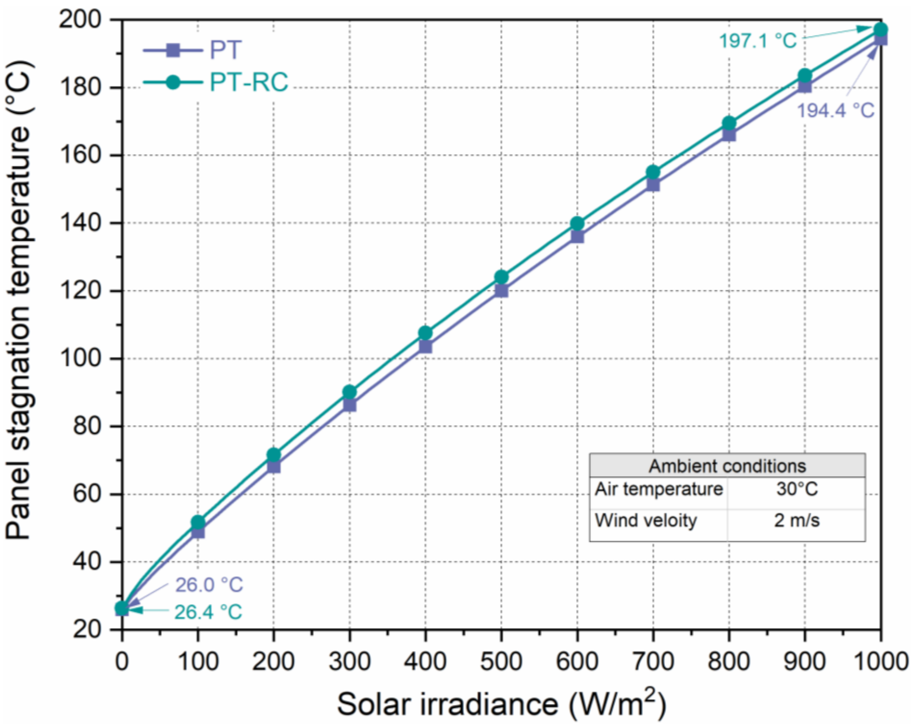

Fig. 6. Panel stagnation temperature of the PT and PT-RC modules in the solar heating mode under different solar irradiances. The ambient temperature and wind velocity are respectively set at 30 °C and 2 m/s.

4.2. Radiative cooling mode

Then, the radiative cooling performance of the PT, RC, and PT-RC modules is investigated and compared. The radiative emitter side of the PT-RC module is up-turned in this operation mode. The cooling power and the stagnation temperature under different solar irradiances are taken as two performance indicators. The ambient temperature and wind velocity are respectively set at 30 °C and 2 m/s as well.

Fig. 7 shows the cooling power of the three modules working at night (solar irradiance equals zero) with different panel temperatures. All three modules have less cooling power at decreased panel temperature as more heat flows into the module through the insulation layer. The RC and PT-RC modules show rather close cooling performance. In particular, they have the same cooling power (69.9 W/m^2) when the panel temperature is equal to the ambient temperature (30 °C). However, as the panel temperature drops continuously, the PT-RC module shows increasing superiority in cooling performance as the air gap between the panel and insulation layer serves as an additional thermal insulator. The panel stagnation temperature of the PT-RC module is 18.3 °C, which is 0.4 °C lower than that of the RC module and 11.7 °C below the ambient temperature. The PT module, on the other hand, presents much less cooling capacity compared to the rest two modules. The long-wave emissivity of the PT panel and the long-wave transmittance of the glass cover are extremely low, indicating that only a very small amount of heat can be radiatively dissipated from the PT panel to the sky.

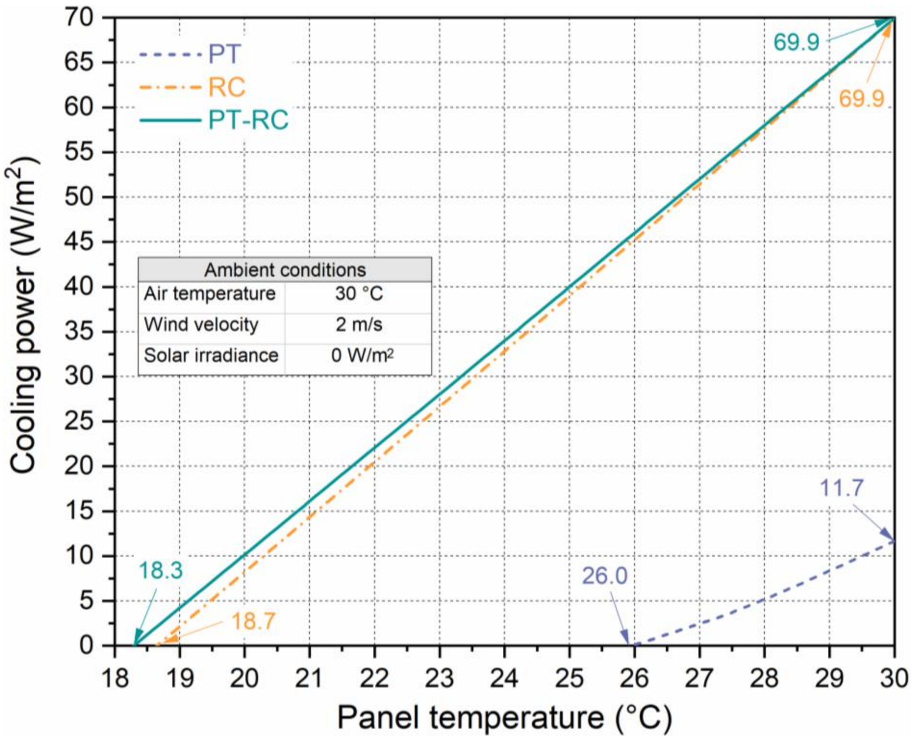

Fig. 7. Cooling power of the PT, RC, and PT-RC modules under different panel temperatures. The ambient temperature, wind velocity, and solar irradiance are respectively set at 30 °C, 2 m/s, and 0 W/m^2.

The panel stagnation temperature of the RC and PT-RC modules in the radiative cooling mode under different solar irradiances is further investigated, as shown in Fig. 8 (results of the PT module have shown in Fig. 6). As the solar irradiance goes up, the panel stagnation temperature of both modules increases almost linearly but is still about 2.5 °C below the ambient temperature even if the solar irradiance reaches 1000 W/m^2, indicating that the two modules can realize daytime radiative cooling in most cases. Besides, the stagnation temperature gap between the RC and PT-RC panels is 0.4 °C when there is no solar irradiance, but shrinks to 0.1 °C when the solar irradiance reaches 1000 W/m^2. It is also because that, with the help of the air gap below the PT-RC panel, the PT-RC module shows increasingly superiority in cooling performance at greater panel-ambient temperature gap.

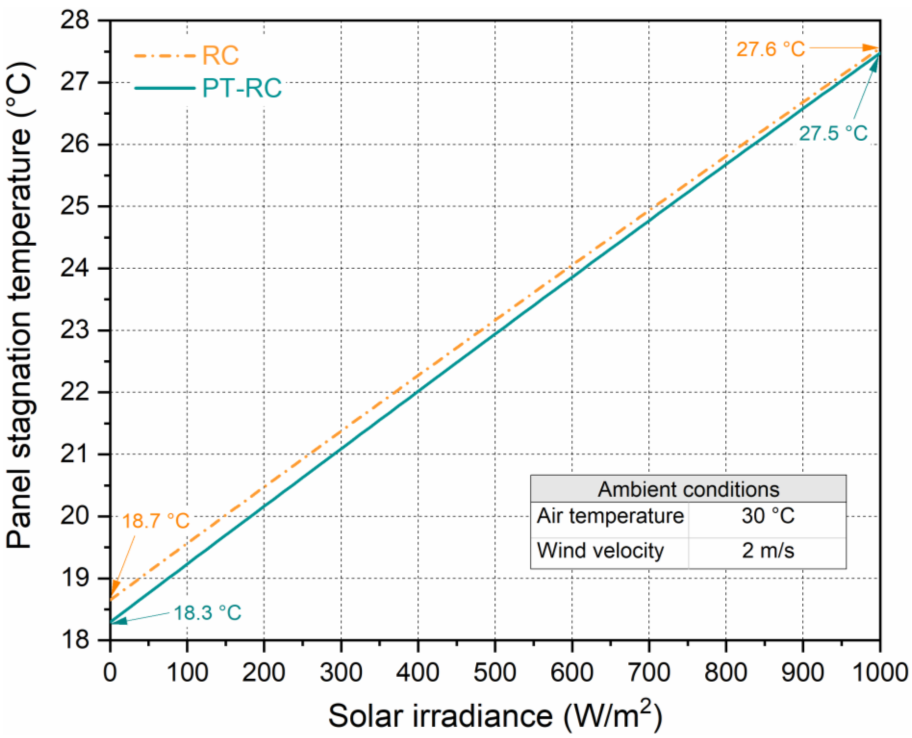

Fig. 8. Panel stagnation temperature of the RC and PT-RC modules in the radiative cooling mode under different solar irradiances. The ambient temperature and wind velocity are respectively set at 30 °C and 2 m/s.

Table 2 compares the performance indicators of the bifacial PT-RC module with other three typical modules reported in the literature. The solar thermal efficiency and net radiative cooling power of the bifacial PT-RC module are comparable to the typical PT collector and RC device, respectively, but greater than those of the spectrally coupled PT-RC module due to the superiority in spectral properties.

Table 2. Thermal performance of different solar heating and/or radiative cooling modules.

Module type	Solar thermal efficiency (T_p = T_a)	Net radiative cooling power (W/m^2)
PT [8]	65.5% – 93.3%	/
RC [31, 32]	/	20 – 127
Spectrally coupled PT-RC [15]	78.3%	41.0
Bifacial PT-RC (This work)	83.3%	69.9

4.3. All-day thermal performance

The all-day heating and cooling performance of the PT-RC module is further studied employed the real weather data in Hefei, China. The solar heating mode starts at 08:00 and ends at 16:00, and the period of radiative cooling mode is from 18:00 to 06:00. The measured solar irradiance, ambient temperature, and wind velocity from October 30th to 31th, 2020 are shown in Fig. 9. The average solar irradiance in solar heating mode (from 08:00 to 16:00) is 637.1 W/m^2, and the average ambient temperature and wind velocity during the whole period are respectively 18.6 °C and 1.3 m/s.

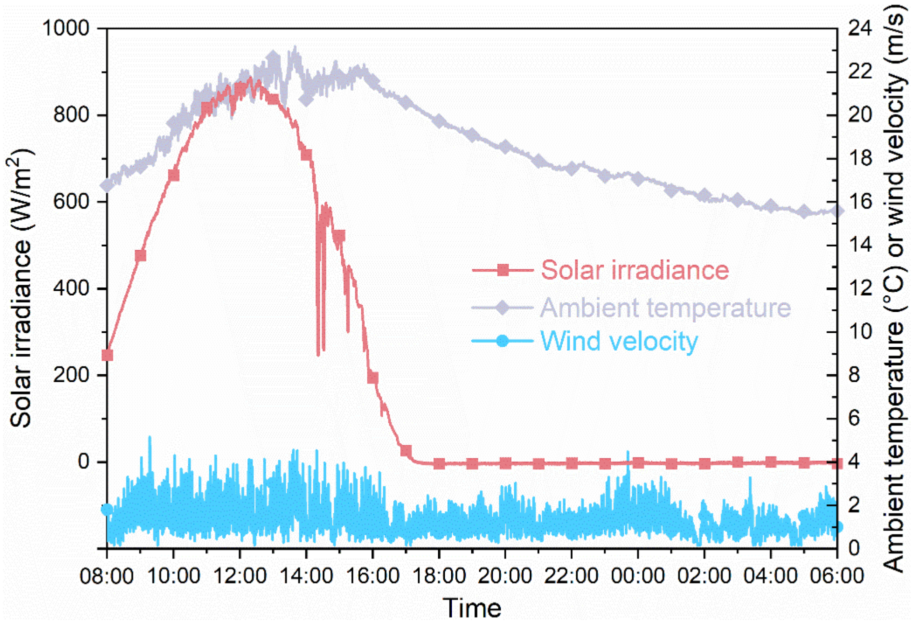

Fig. 9. Measured solar irradiance, ambient temperature, and wind velocity from 08:00, October 30th to 06:00, October 31st, 2020 in Hefei, China.

Fig. 10 presents the heat and cooling powers of the three modules during the day. In this case study, the panel temperature is set equal to the ambient temperature, and thus the net solar heating and net radiative cooling powers are calculated as the performance indicators. During the solar heating mode, namely, from 08:00 to 16:00, the PT and PT-RC modules show good thermal-collection performance, with the average heating power being 490.5 and 528.5 W/m^2, respectively. In contrast, attributed to the extremely high solar reflectance and long-wave emissivity of the RC panel, the RC module delivers cooling power even at noon when the solar irradiance exceeds 800 W/m^2. An average cooling flux of 25.8 W/m^2 indicates that the RC module has favorable daytime radiative cooling performance. During the radiative cooling mode, namely, from 18:00 to 06:00, the RC and PT-RC modules exhibit the same cooling power as there is no non-radiative cooling loss for both modules when the panel temperature equals that of the ambient air. The average cooling power of the two modules during the consecutive 12 hours is 58.0 W/m^2, while that of the PT module is only 12.3 W/m^2 due to its unfavorable spectral property for radiative cooling. Table 3 further shows the heat and cooling energy gains of the three modules during the day, suggesting that the PT-RC module offers the best overall heating and cooling performance among the three devices.

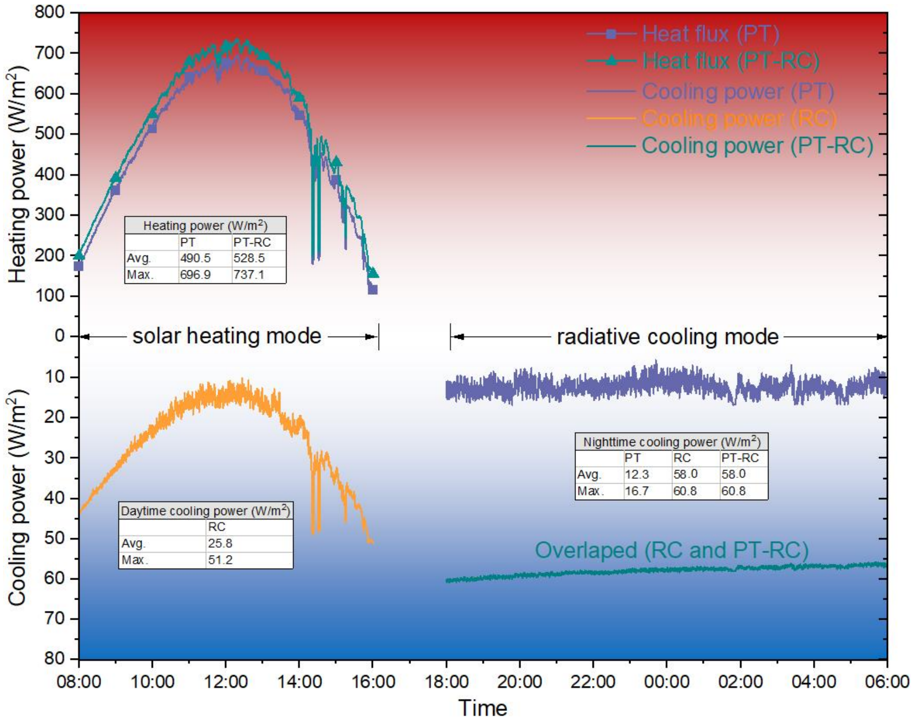

Fig. 10. Heating and cooling powers of the PT, RC, and PT-RC modules from 08:00, October 30th to 06:00, October 31st, 2020 in Hefei, China. The panel temperature is set equal to the ambient temperature.

Table 3. Energy gains of three modules from 08:00, October 30th to 06:00, October 31st, 2020 in Hefei, China.

Module type	Heat (MJ)	Cooling energy (MJ)	Total (MJ)
PT	15.0	0.5	15.5
RC	0	3.3	3.3
PT-RC	15.2	2.5	17.7

5. Conclusions

In summary, by coating the backside of the solar absorber with the radiative cooling material, a bifacial solar photothermic and radiative cooling (PT-RC) module is developed. The bifacial panel faces the sun with its solar absorber side for thermal-collection, and can flexibly switch to radiative cooling mode by upturning the radiative emitter side when cooling energy is required. The solar thermal efficiency of the PT-RC module reaches 83.3% at zero-reduced temperature under given conditions, which is even slightly better than that of the typical PT module due to the existence of the air gap below the panel and the low long-wave emissivity of the PE cover. The net radiative cooling power of the PT-RC module under certain conditions is 69.9 W/m^2, which is equal to that of the RC module and about six times that of the PT module. In addition, backed by the air gap below the panel and favorable spectral property for radiative cooling, the PT-RC module shows the lowest panel stagnation temperature among the three modules, with the value being 11.7 °C lower than the ambient temperature. On a typical day in Hefei, the PT-RC gains 15.2 MJ heat and 2.5 MJ cooling energy. In contrast, those of the PT module are respectively 15.0 MJ and 0.5 MJ, while the RC module has no solar heating capacity and only provides 3.3 MJ cooling energy. Compared to the stand-alone PT and RC modules, the PT-RC module shows advantages in terms of multi-function, flexibility, seasonal adaptability, and overall efficiency, etc. As heating and cooling demands are constantly changing in the real world, this bifacial module shows great potential in energy saving and smart thermal management. Future studies will focus on devising a full-scale bifacial PT-RC and testing its outdoor heating and cooling performance, as well as evaluating its potential in building energy saving.

Acknowledgments

This study was sponsored by the National Key R&D Program of China (2018YFD0700200), H2020 Marie Skłodowska-Curie Actions - Individual Fellowships (842096), National Natural Science

Foundation of China (NSFC 51906241 and 51776193), and Anhui Provincial Natural Science Foundation (1908085ME138).

Appendix

This appendix is arranged to clearly show the mathematical model described in Section 3.

- *Wind screen*

In Eq. (1), α_w is the absorptivity of the wind screen in solar radiation band; G is the solar irradiance, W/m^2; h_{aw} and h_{wp} are correspondingly the overall heat transfer coefficient between the ambient air and wind screen and that between the wind screen and absorber/emitter panel, W/(m^2·K); h_{sw} is the radiative heat transfer coefficient between the sky and wind screen (RC and PT-RC modules), W/(m^2·K); T_a, T_w, T_p, and T_s are respectively the temperature of the ambient air, wind screen, absorber/emitter panel, and sky, K. Q_{rad_sw} is the net radiative thermal flux from the wind screen (PT module) to the sky, W/m^2.

The overall heat transfer coefficient between the ambient air and wind screen is expressed as [33]:

$$h_{aw} = 2.8 + 3.0u_a \tag{A1}$$

where u_a is the wind velocity, m/s.

The overall heat transfer coefficient between the wind screen and absorber/emitter panel is made up of convective and radiative heat transfer coefficients, described as:

$$h_{wp} = \frac{Nu \cdot k_a}{d_{wp}} + \frac{\sigma\left(T_w^2 + T_p^2\right)\left(T_w + T_p\right)}{1/\varepsilon_w + 1/\varepsilon_p - 1} \tag{A2}$$

where Nu is the Nusselt number; k_a is the thermal conductivity of air, W/(m·K); d_{wp} is the height of the air gap between the wind screen and absorber/emitter panel, m; σ is the Stefan–Boltzmann constant,

5.67×10^{-8} W/m$^2\cdot$K^4; and ε_w and ε_p are respectively the total, hemispherical emissivity of the wind screen and absorber/emitter panel.

The radiative heat transfer coefficient between the sky and wind screen (RC and PT-RC modules) is written as:

$$h_{sw} = \varepsilon_w \sigma \left(T_s^2 + T_w^2\right)\left(T_s + T_w\right) \tag{A3}$$

The net radiative thermal flux from the wind screen (PT module) to the sky is the outward thermal radiation of the wind screen subtracting the thermal emission absorbed by the wind screen from the sky, expressed as [34]:

$$\begin{aligned} Q_{rad\_sw} &= \varphi\left(Q_{w\_rad} - Q_{s\_rad}\right) \\ &= \varphi\left(\varepsilon_w \int_{0.3}^{25} E_{b,\lambda}\left(\lambda, T_w\right) d\lambda - \alpha_w \int_{0.3}^{25}\int_0^{\pi/2} \varepsilon_{s,\lambda}\left(\lambda,\theta\right) E_{b,\lambda}\left(\lambda, T_a\right) \sin\theta \cos\theta d\theta d\lambda\right) \end{aligned} \tag{A4}$$

where φ is the inclination angle factor, which is 0.85 in this work [35]; $E_{b,\lambda}$ denotes the spectral radiant power of the blackbody, W/(m$^2\cdot$μm); α_w is the total, hemispherical absorptivity of the wind screen; $\varepsilon_{s,\lambda}(\lambda,\theta)$ refers to the spectral, directional emissivity of the sky; λ is the wavelength, μm; θ is the zenith angle, rad; and $\alpha_{w,\lambda}(\lambda,\theta)$ is the spectral, directional absorptivity of the wind screen.

$\varepsilon_{s,\lambda}(\lambda,\theta)$ is calculated as [11]:

$$\varepsilon_{s,\lambda}\left(\lambda,\theta\right) = 1 - \tau_{s,\lambda}\left(\lambda, 0\right)^{1/\cos\theta} \tag{A5}$$

where $\tau_{s,\lambda}(\lambda,\theta)$ is the transmittance of the atmosphere in the zenith direction.

- *Absorber/emitter panel*

In Eq. (2), α_p is the absorptivity of the panel in solar radiation band; U_{ap} is the overall heat transfer coefficient between the panel and ambient air, W/(m$^2\cdot$K); Q_{rad_sp} is the net radiative thermal flux from the panel (RC and PT-RC modules) to the sky, W/m^2; h_{pi} is the overall heat transfer coefficient between the panel and insulation layer, W/(m$^2\cdot$K). T_i is the temperature of the upper surface of the insulation layer, K. Q_{gain} is the heat ("–" sign) or cooling energy ("+" sign) extracted from the panel, W/m^2. Q_{gain} is zero when the panel reaches its stagnation temperature.

The overall heat transfer coefficient between the panel (PT and RC modules) and ambient air is expressed as:

$$U_{ap} = \frac{1}{d_i / k_i + 1/h_{ai}} \quad \text{(A6)}$$

Where d_i and k_i are respectively the thickness and thermal conductivity of the thermal insulation layer, m and W/(m·K); and h_{ai} is the convective heat transfer coefficient between the ambient air and insulation layer, which equals h_{aw} in expression.

The net radiative thermal flux from the panel (PT-RC module) to the sky is expressed as:

$$\begin{aligned} Q_{rad\_sp} &= \varphi\left(Q_{p\_rad} - Q_{s\_rad}\right) \\ &= \varphi\tau_w\left(\varepsilon_p\int_{0.3}^{25} E_{b,\lambda}\left(\lambda, T_p\right)\mathrm{d}\lambda - \alpha_p\int_{0.3}^{25}\int_0^{\pi/2}\varepsilon_{s,\lambda}\left(\lambda,\theta\right)E_{b,\lambda}\left(\lambda, T_a\right)\sin\theta\cos\theta\,\mathrm{d}\theta\,\mathrm{d}\lambda\right) \end{aligned} \quad \text{(A7)}$$

where τ_w is the total, hemispherical transmittance of the wind screen; and α_p is the total, hemispherical absorptivity of the panel.

- *Insulation layer*

In Eq. (3), U_{ai} is the overall heat transfer coefficient between the upper surface of the insulation layer and ambient air, W/(m^2·K), and its expression equals that of the U_{ap}.

Nomenclature

d: thickness, m
E: radiant power, W/(m^2·μm)
G: solar irradiance, W/m^2
h: heat transfer coefficient, W/(m^2·K)
k: thermal conductivity, W/(m·K)
Nu: Nusselt number, -
Q: heat flux, W/m^2
T: temperature, K or °C

U: overall heat transfer coefficient, W/(m^2·K)
u: wind velocity, m/s
τ: transmittance, -
α: absorptivity, -
ε: emissivity, -
σ: Stefan–Boltzmann constant, 5.67×10^{-8} W/m$^2 \cdot$ K^4
φ: inclination angle factor, -
λ: wavelength, μm
θ: zenith angle, rad

Abbreviation and subscripts
a: ambient
b: blackbody
i: insulation layer
p: panel
rad: radiation
s: sky
w: wind screen

References

[1] Raja AA, Huang Y. Novel parabolic trough solar collector and solar photovoltaic/thermal hybrid system for multi-generational systems. Energy Convers Manage 2020;211:112750.

[2] Aili A, Zhao D, Lu J, Zhai Y, Yin X, Tan G, et al. A kW-scale, 24-hour continuously operational, radiative sky cooling system: Experimental demonstration and predictive modeling. Energy Convers Manage 2019;186:586-96.

[3] Ning Y, Wang C, Wang W, Tomasella E, Sun Y, Song P, et al. Improvement of thermal stability of ZrSiON based solar selective absorbing coating. J Materiomics 2020;6:760-7.

[4] Zhao B, Hu M, Ao X, Chen N, Pei G. Radiative cooling: A review of fundamentals, materials, applications, and prospects. Appl Energy 2019;236:489-513.

[5] Agathokleous R, Barone G, Buonomano A, Forzano C, Kalogirou SA, Palombo A. Building façade integrated solar thermal collectors for air heating: experimentation, modelling and applications. Appl Energy 2019;239:658-79.

[6] Yi Z, lv Y, Xu D, Xu J, Qian H, Zhao D, et al. Energy saving analysis of a transparent radiative cooling film for buildings with roof glazing. Energy Built Environ 2020.

[7] Zhao D, Yin X, Xu J, Tan G, Yang R. Radiative sky cooling-assisted thermoelectric cooling system for building applications. Energy 2020;190:116322.

[8] Li X, Sun B, Sui C, Nandi A, Fang H, Peng Y, et al. Integration of daytime radiative cooling and solar heating for year-round energy saving in buildings. Nat Commun 2020;11:6101.

[9] Zhao B, Hu M, Ao X, Chen N, Xuan Q, Su Y, et al. A novel strategy for a building-integrated diurnal photovoltaic and all-day radiative cooling system. Energy 2019;183:892-900.

[10] Ono M, Chen K, Li W, Fan S. Self-adaptive radiative cooling based on phase change materials. Opt Express 2018;26:A777-A87.

[11] Raman AP, Anoma MA, Zhu L, Rephaeli E, Fan S. Passive radiative cooling below ambient air temperature under direct sunlight. Nature 2014;515:540-4.

[12] Yang Y, Long L, Meng S, Denisuk N, Chen G, Wang L, et al. Bulk material based selective infrared emitter for sub-ambient daytime radiative cooling. Sol Energy Mater Sol Cell 2020;211:110548.

[13] Ao X, Hu M, Zhao B, Chen N, Pei G, Zou C. Preliminary experimental study of a specular and a diffuse surface for daytime radiative cooling. Sol Energy Mater Sol Cell 2019;191:290-6.
[14] Huang Z, Ruan X. Nanoparticle embedded double-layer coating for daytime radiative cooling. Int J Heat Mass Tran 2017;104:890-6.
[15] Hu M, Zhao B, Ao X, Su Y, Wang Y, Pei G. Comparative analysis of different surfaces for integrated solar heating and radiative cooling: A numerical study. Energy 2018;155:360-9.
[16] Frattolillo A, Loddo G, Mastino CC, Baccoli R. Heating and cooling loads with electrochromic glazing in Mediterranean climate. Energy Build 2019;201:174-82.
[17] Taylor S, Long L, McBurney R, Sabbaghi P, Chao J, Wang L. Spectrally-selective vanadium dioxide based tunable metafilm emitter for dynamic radiative cooling. Sol Energy Mater Sol Cell 2020;217:110739.
[18] Mandal J, Jia M, Overvig A, Fu Y, Che E, Yu N, et al. Porous Polymers with Switchable Optical Transmittance for Optical and Thermal Regulation. Joule 2019;3:3088-99.
[19] Wang W, Zhao Z, Zou Q, Hong B, Zhang W, Wang GP. Self-adaptive radiative cooling and solar heating based on a compound metasurface. J Mater Chem C 2020;8:3192-9.
[20] Chen Z, Zhu L, Li W, Fan S. Simultaneously and Synergistically Harvest Energy from the Sun and Outer Space. Joule 2019;3:101-10.
[21] Liu J, Zhou Z, Zhang D, Jiao S, Zhang J, Gao F, et al. Research on the performance of radiative cooling and solar heating coupling module to direct control indoor temperature. Energy Convers Manage 2020;205:112395.
[22] Matsuta M, Terada S, Ito H. Solar heating and radiative cooling using a solar collector-sky radiator with a spectrally selective surface. Sol Energy 1987;39:183-6.
[23] Hu M, Pei G, Wang Q, Li J, Wang Y, Ji J. Field test and preliminary analysis of a combined diurnal solar heating and nocturnal radiative cooling system. Appl Energy 2016;179:899-908.
[24] Hu M, Zhao B, Ao X, Su Y, Pei G. Parametric analysis and annual performance evaluation of an air-based integrated solar heating and radiative cooling collector. Energy 2018;165:811-24.
[25] Kort-Kamp WJM, Kramadhati S, Azad AK, Reiten MT, Dalvit DAR. Passive Radiative “Thermostat” Enabled by Phase-Change Photonic Nanostructures. ACS Photonics 2018;5:4554-60.
[26] Parsons AM, Sharp K. Design parameters and control strategies for a combined passive heating and cooling system in Louisville, KY. Int J Sustain Energy 2019;38:981-1001.
[27] Hu M, Zhao B, Ao X, Chen N, Cao J, Wang Q, et al. Feasibility research on a double-covered hybrid photo-thermal and radiative sky cooling module. Sol Energy 2020;197:332-43.
[28] Hsu P-C, Liu C, Song AY, Zhang Z, Peng Y, Xie J, et al. A dual-mode textile for human body radiative heating and cooling. Sci Adv 2017;3:e1700895.
[29] Zaaoumi A, Asbik M, Hafs H, Bah A, Alaoui M. Thermal performance simulation analysis of solar field for parabolic trough collectors assigned for ambient conditions in Morocco. Renew Energy 2021;163:1479-94.
[30] Liu J, Zhang J, Zhang D, Jiao S, Zhou Z, Tang H, et al. Theoretical and experimental research towards the actual application of sub-ambient radiative cooling. Sol Energy Mater Sol Cell 2021;220:110826.
[31] Cavelius R, Isaksson C, Perednis E, Read GE. Passive cooling technologies. Austrian Energy Agency. 2005:125.
[32] Kou J-l, Jurado Z, Chen Z, Fan S, Minnich AJ. Daytime Radiative Cooling Using Near-Black Infrared Emitters. ACS Photonics. 2017;4:626-30.
[33] Hu M, Zhao B, Ao X, Ren X, Cao J, Wang Q, et al. Performance assessment of a trifunctional system integrating solar PV, solar thermal, and radiative sky cooling. Appl Energy 2020;260:114167.
[34] Hu M, Zhao B, Ao X, Suhendri, Cao J, Wang Q, et al. An analytical study of the nocturnal radiative cooling potential of typical photovoltaic/thermal module. Appl Energy 2020;277:115625.
[35] Erell E, Etzion Y. Heating experiments with a radiative cooling system. Build Environ 1996;31:509-17.